

# **Significance of Biological H<sub>2</sub> Oxidation in a Continuous Single-Chamber Microbial Electrolysis Cell**

Hyung-Sool Lee<sup>\*</sup>, and Bruce E. Rittmann

Center for Environmental Biotechnology, The Biodesign Institute at Arizona State University, 1001 S. McAllister Ave. Tempe, AZ 85287-5701, USA

\*Corresponding author: Tel.: +1-480-727-0849; Fax: +1-480-727-0889

E-mail addresses: [hyungsool@asu.edu](mailto:hyungsool@asu.edu) (H.S. Lee), [Rittmann@asu.edu](mailto:Rittmann@asu.edu) (B.E. Rittmann)

7 figures, 1 table, and 11 pages

## 1. A Schematic Diagram of the Upflow Single-Chamber MEC

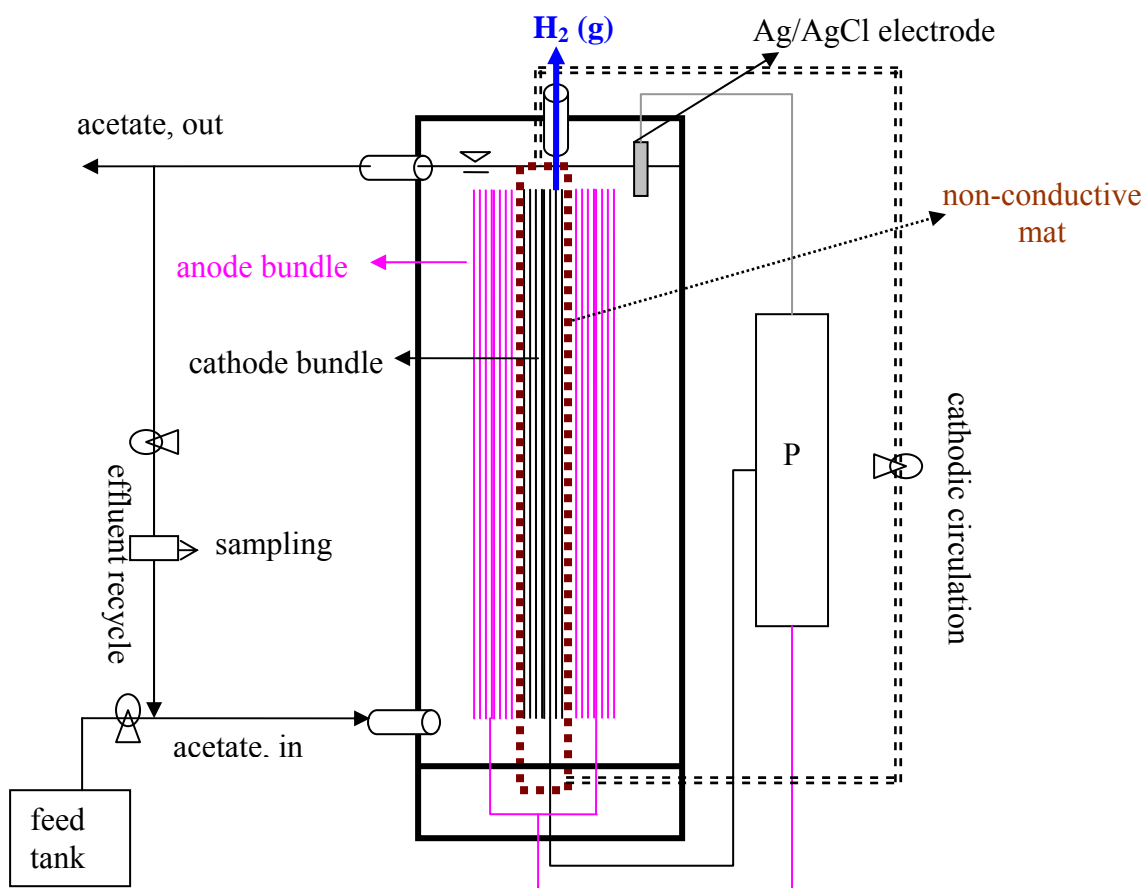


Figure S1. Schematic diagram of the upflow single-chamber MEC using graphite-fiber bundles as electrodes. P – a potentiostat for power supply. We separated the cathode bundle from the anodes using a non-conductive mat.

## 2. An Equivalent Circuit

To measure ohmic resistance in the single-chamber microbial electrolysis cell (MEC), we performed electrochemical impedance spectroscopy (EIS) using a potentiostat. We analyzed impedance spectra at a fixed anode potential = +0.07V (vs. SHE) for a closed-circuit system. We varied the frequency from 100 kHz to 10 mHz with an alternating-current signal of 10 mV amplitude. We recorded the impedance spectra when the anode was the working electrode, the cathode was the counter electrode, and Ag/AgCl was the reference electrode. We analyzed EIS data with an electrical circuit (Figure S2) that is comprised of an ohmic-resistance component and a constant-phase element in parallel with a resistance combining charge-transfer with diffusion. To accurately estimate ohmic resistance, we fit the EIS data with a Levenberg-Marquardt non-linear least square algorithm in EC lab software (Version 9.5).

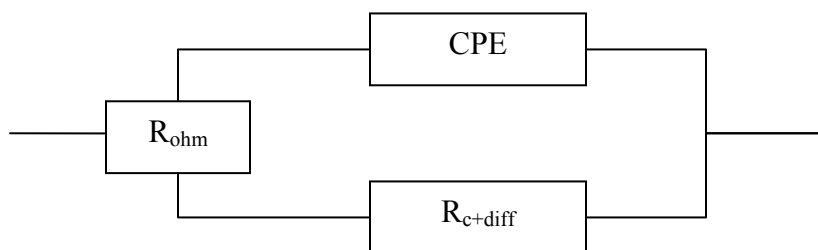


Figure S2. An equivalent circuit used for impedance analyses.  $R_{ohm}$ : ohmic resistance, CPE is a double layer constant phase element, and  $R_{c+diff}$  is sum of charge transfer resistance and diffusion resistance.

### 3. Measurement of Dissolved H<sub>2</sub> Concentration

We measured dissolved H<sub>2</sub> concentration in the steady-state continuous MEC in order to quantify H<sub>2</sub> loss from effluent discharge. We directly sampled 1 mL of liquid from the MEC with a sterile syringe and moved the sample into a 5-mL glass tube capped with butyl rubber stopper that had been sparged with ultrapure N<sub>2</sub> gas (99.999%) for 30 min. Then, we placed the glass tube in a 30°C incubation shaker for 3 days to establish equilibrium between liquid and gas phases; we carried out control test with the glass tube in the same condition without injecting liquid sample and used its measured H<sub>2</sub> gas concentration as the blank. We quantified H<sub>2</sub> gas concentration in headspace with a trace analytical gas chromatograph (ta 3000, Ametek) using a reduction gas detector and ultra purity N<sub>2</sub> (99.999%) as a carrier gas at a pressure of 90 psig. Standard H<sub>2</sub> gas (100 ppm, Matheson Trigas) was used for establishing calibration curves by blending with N<sub>2</sub>. We measured dissolved H<sub>2</sub> concentration of the MEC in duplicate for each HRT.

#### 4. Gas Composition in the Single-chamber MEC.

We monitored gas composition in the continuous single-chamber MEC. Figure S3 shows that H<sub>2</sub> gas composition was very stable at 49-53%, and CH<sub>4</sub> fraction of gas was small at 1.8-6.9% with HRT varied. The small, but consistent CH<sub>4</sub> production, despite the short HRT, suggests accumulation of methanogens on the electrodes, which means that we cannot suppress methanogenesis in a continuous single-chamber MEC by controlling hydraulic retention time.

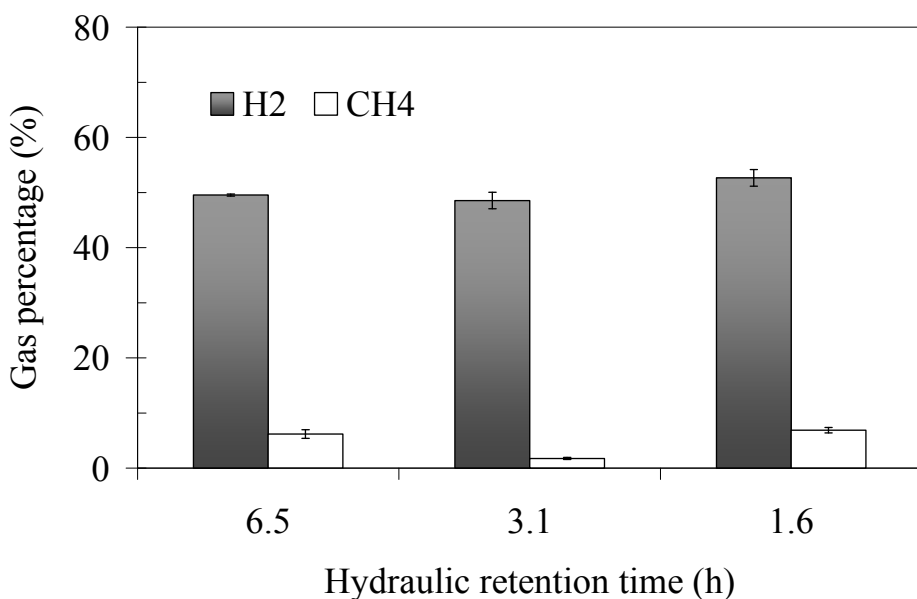


Figure S3. Percentages of H<sub>2</sub> and CH<sub>4</sub> gases in the single-chamber MEC for different HRTs.

## 5. Characterization of Current Density from Acetate and H<sub>2</sub>.

We estimated distributions of current density produced from acetate and H<sub>2</sub> given that the true coulombic efficiency (CE) for acetate is 90%, which is close to the maximum CE reported from MFC/MEC studies (*1*). To characterize current density, we subtracted 0.9 times the current density associated with acetate utilization from the observed current density for quantifying the current density from H<sub>2</sub> oxidation. As seen in Figure S4, the current density from acetate oxidation was 47%, 40%, and 29% of observed current density, respectively, for HRT 1.6, 3.1, and 6.5 h. This characterization supports that anode-respiring bacteria in our single-chamber MEC preferred H<sub>2</sub> to acetate as electron donor and that the H<sub>2</sub> recycle effect was very significant for current generation.

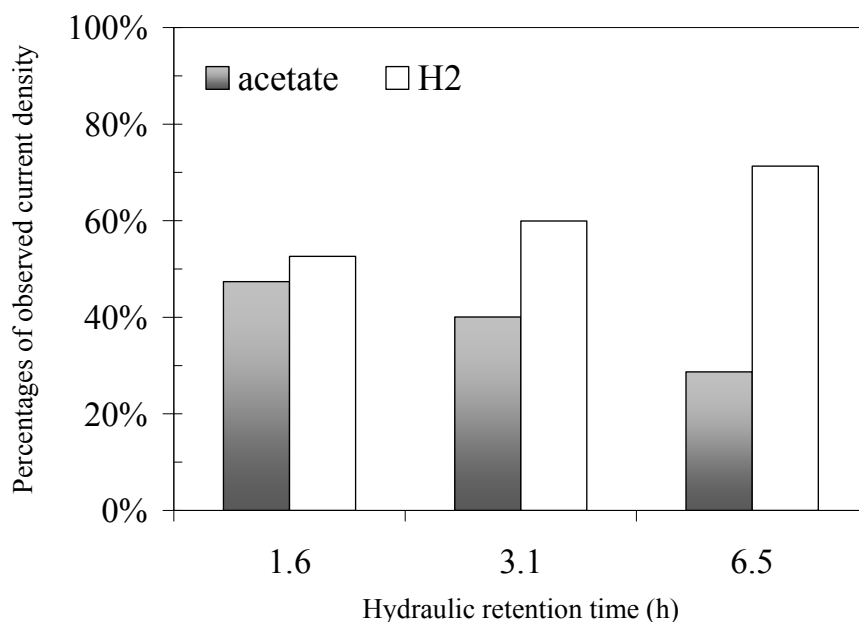


Figure S4. Distributions of coulombs generated from acetate and H<sub>2</sub> in the single MEC given that CE is 90% for acetate.

## 6. Quantification of Ohmic Resistance

Figure S5 presents Nyquist plots in duplicate experiments at HRT 1.6 h and anode potential  $-0.03\text{ V}$  (vs standard hydrogen electrode). Read values of ohmic resistance were  $\sim 0.38\ \Omega$ , but average of ohmic resistances estimated by the Levenberg-Marquardt non-linear least square algorithm using EC lab software were  $0.49\ \Omega$ . Either result supports that eliminating membrane from MEC systems can almost totally eliminate ohmic resistance.

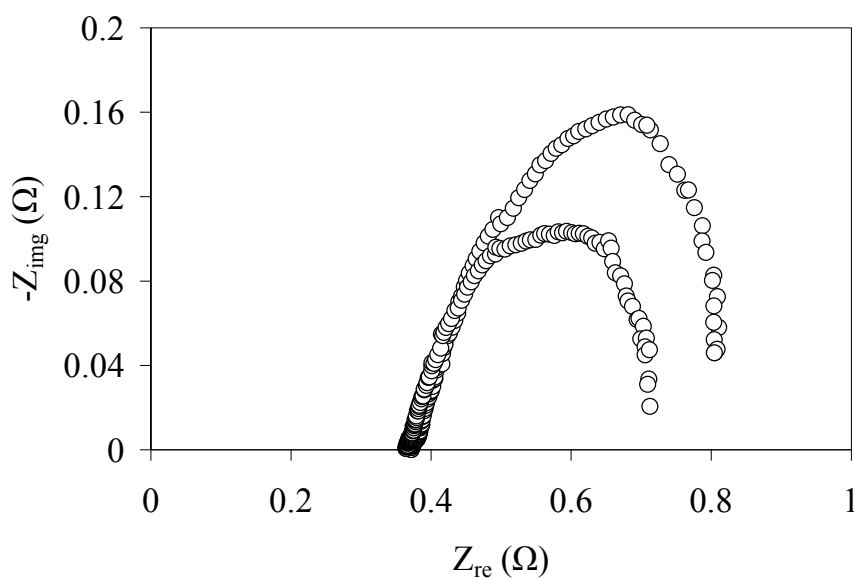
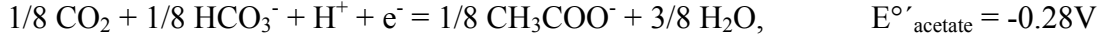


Figure S5. Nyquist plots for the single MEC operated at 1.6 h of HRT and  $E_{\text{anode}}$  fixed at  $-0.03\text{ V}$ . Current was  $0.195\text{--}0.208\text{ A}$  ( $1,560\text{--}1,662\text{ A/m}^3$ ).

## 7. Characterization of Anode and Cathode Over-potentials.

We computed anode and cathode over-potentials, based on standard potential for reducing half-reactions for acetate and water at pH 7.

The anode reaction for acetate oxidation is:



The cathode reaction for water molecule reduction is:



Anode over-potential ( $\eta_{\text{anode}}$ ) can be computed by the relation of  $\eta_{\text{anode}} = \text{anode potential} - E^{\circ'}_{\text{acetate}}$ . Due to a fixed anode potential at -0.126 V vs. SHE, anode over-potential was calculated by

$$\text{Anode over-potential} = (-0.126) - (-0.28) = 0.154 \text{ V}$$

Cathode over-potential ( $\eta_{\text{cathode}}$ ) was calculated by the relation of  $\eta_{\text{cathode}} = E^{\circ'}_{\text{H}_2\text{O}} - \text{cathode potential}$ . Since cathode potentials varied with current density in our experiments, cathode over-potential changed slightly with HRT. We summarize all over-potentials and applied voltage for each HRT in Table S1.



Table S1. Characterization of electrode over-potentials, ohmic energy losses, and measured applied voltage for each HRT

HRT (h)	$\eta_{\text{anode}}$ (V)	$\eta_{\text{cathode}}$ (V)	$\eta_{\text{ohmic}}$ (V)	Applied voltage (V)
6.5	0.154	$1.15 \pm 0.07$	$0.090 \pm 0.003$	$1.43 \pm 0.04$
3.1	0.154	$1.19 \pm 0.05$	$0.097 \pm 0.002$	$1.47 \pm 0.05$
1.6	0.154	$1.21 \pm 0.03$	$0.1 \pm 0.003$	$1.49 \pm 0.03$

$\eta_{\text{anode}}$ : anode over-potential (V),  $\eta_{\text{cathode}}$ : cathode over-potential (V), and  $\eta_{\text{ohmic}}$ : ohmic energy loss (V).

Total energy losses were computed to be 1.39 V – 1.46 V, while total energy losses range from 1.3V – 1.4V, based on theoretical standard potential of 0.13 V for  $\text{CH}_3\text{COO}^- + 3 \text{H}_2\text{O} = \text{CO}_2 + \text{HCO}_3^- + 4 \text{H}_2$  at pH 7. A small error ( $\sim 0.1$  V) can occur because we did not account for temperature and constituents' concentration in these computations. Characterization of over-potentials and ohmic energy losses clearly shows that cathode over-potential was the main energy loss in our single-chamber MEC lacking metal catalyst on the cathode.

## 8. Estimation of H<sub>2</sub> Production Rate to Applied Voltage at CCE = 100%

We calculated H<sub>2</sub> production rate from the single-chamber MEC given that no H<sub>2</sub> recycle and methanogenesis occur in the MEC (CCE=100%). To provide current density data for different applied voltages, we decreased anode potential from -0.126 to -0.326 V (vs. standard hydrogen electrode) in a potentiostat mode. For steady-state acetate concentration, we converted average of current density into H<sub>2</sub> production rate at each applied voltage. Using linear regression, we obtained the equation  $y = 15.632x - 5.0988$  where  $y$  is H<sub>2</sub> production rate (m<sup>3</sup> H<sub>2</sub>/m<sup>3</sup>-d) and  $x$  is applied voltage (V).

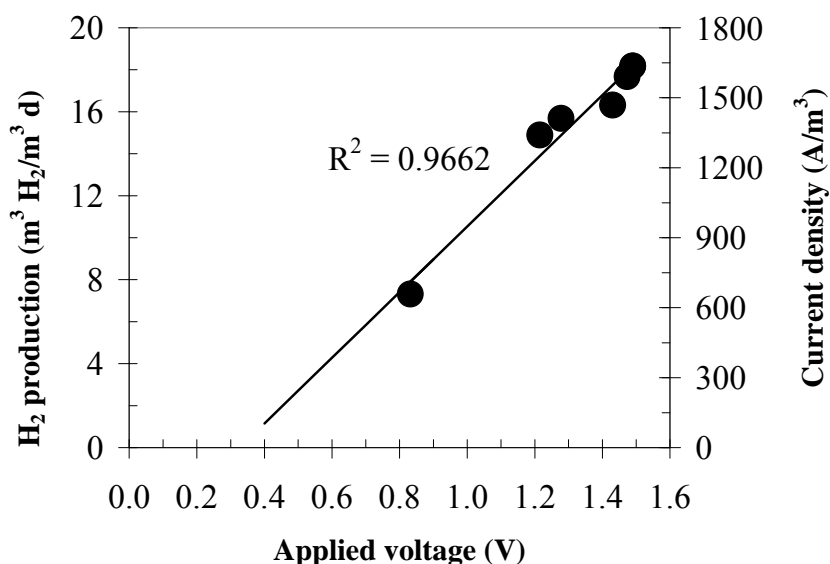


Figure S6. Linear regression for H<sub>2</sub> production rate (volumetric current density) and applied voltage at CCE (cathodic conversion efficiency) of 100%.

Figure S7 compares the estimated and observed  $\text{H}_2$ -production rates against the applied voltage. Applied voltage required for generating  $4.32 \text{ m}^3 \text{ H}_2/\text{m}^3\text{-d}$  is only 0.6 V, while observed applied voltage for this  $\text{H}_2$  production was 1.49 V. This comparison indicates that  $\text{H}_2$  recycle can increase applied voltage up to 0.9 V more than its minimum requirement.

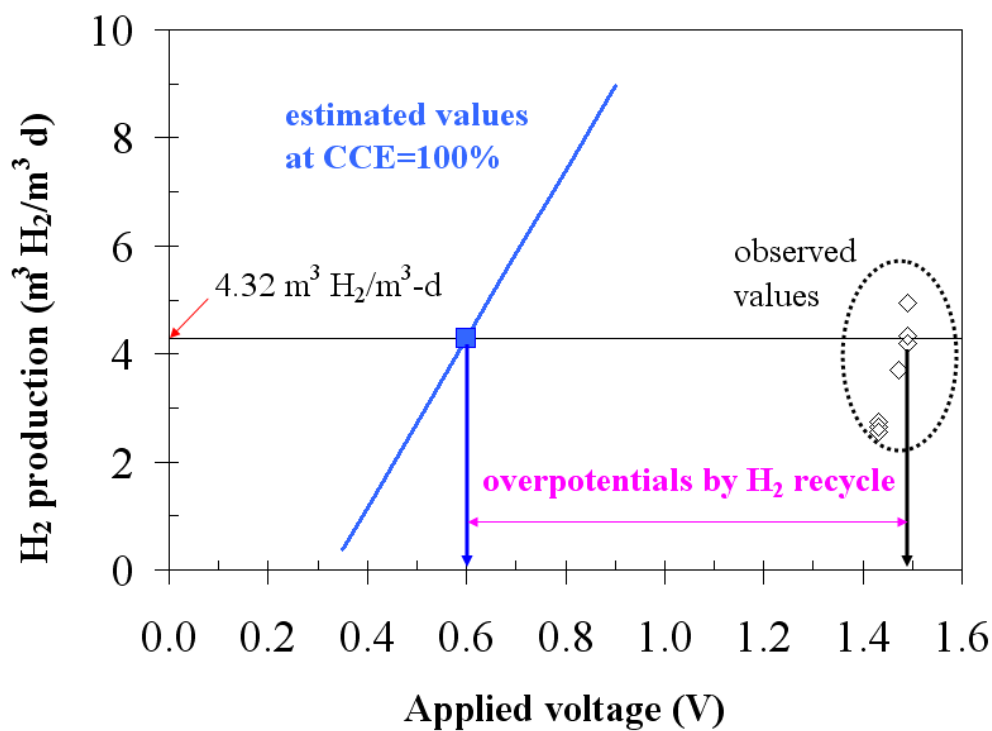


Figure S7. Correlations between  $\text{H}_2$  production rate and applied voltage with and without  $\text{H}_2$  recycle and  $\text{CH}_4$  formation.

### Literature Cited

1. Bond, D. R.; Lovley, D. R. Electricity Production by *Geobacter sulfurreducens* Attached to Electrodes. *Appl. Environ. Microbiol.* **2003**, 69 (3), 1548-1555.